Cyclin D1 Provides a Link between Development and Oncogenesis in the Retina and Breast

Piotr Sicinski,* Joana Liu Donaher,* Susan B. Parker,†
Tiansen Li,‡ Amin Fazeli,* Humphrey Gardner,*
Sandra Z. Haslam,§ Roderick T. Bronson,∥
Stephen J. Elledge,† and Robert A. Weinberg*
*The Whitehead Institute for Biomedical Research
and Department of Biology
Massachusetts Institute of Technology
Cambridge, Massachusetts 02142
†Howard Hughes Medical Institute
Verna and Mars McLean Department of Biochemistry
Baylor College of Medicine
Houston, Texas 77030
‡The Berman–Gund Laboratory
  for the Study of Retinal Degenerations
Harvard Medical School
Massachusetts Eye and Ear Infirmary
Boston, Massachusetts 02114
§Department of Physiology
Michigan State University
East Lansing, Michigan 48824
∥Department of Pathology
Tufts University Schools of Medicine and Veterinary
  Medicine
Boston, Massachusetts 02111

Summary

Mice lacking cyclin D1 have been generated by gene targeting in embryonic stem cells. Cyclin D1-deficient animals develop to term but show reduced body size, reduced viability, and symptoms of neurological impairment. Their retinas display a striking reduction in cell number due to proliferative failure during embryonic development. In situ hybridization studies of normal mouse embryos revealed an extremely high level of cyclin D1 in the retina, suggesting a special dependence of this tissue on cyclin D1. In adult mutant females, the breast epithelial compartment fails to undergo the massive proliferative changes associated with pregnancy despite normal levels of ovarian steroid hormones. Thus, steroid-induced proliferation of mammary epithelium during pregnancy may be driven through cyclin D1.

Introduction

The control of mammalian cell proliferation by extracellular signals occurs largely during the G1 phase of the cell cycle. During this period, growth stimulatory and growth inhibitory signals transduced from the extracellular environment converge on the cell cycle clock operating in the cell nucleus. This apparatus, composed of cyclins and their associated cyclin-dependent kinases (CDKs), may respond by setting into motion an autonomous cell division program that carries the cells through S, G2, and M phases

or, alternatively, by causing exit from the cell cycle into the quiescent G0 state (reviewed by Sherr, 1994).

Once formed and activated in G1, complexes of specific cyclins and CDKs trigger cell cycle progression by phosphorylating critical cellular substrate proteins. Four mammalian G1 cyclins have been enumerated to date: cyclins D1, D2, and D3 (D-type cyclins) and cyclin E. Expression of the D cyclins is rapidly induced upon exposure of cells to mitogens; this expression declines when mitogens are withdrawn or antiproliferative agents are added (reviewed by Sherr, 1994).

Recent studies suggest that the major target of cyclin D-mediated phosphorylation is the retinoblastoma tumor suppressor gene product, pRB. Indeed, pRB may be the only important rate-limiting substrate of cyclin D–CDK complexes, in that the growth of cells lacking pRB no longer requires cyclin D (reviewed by Weinberg, 1995).

In many types of human tumor cells, the expression of cyclin D1 is deregulated, favoring the phosphorylation and functional inactivation of pRB. Indeed, the cyclin D1 gene was originally cloned as an oncogene, termed *PRAD1*, that was found to be activated by chromosomal translocations present in the genomes of parathyroid adenoma cells (Motokura et al., 1991). Consistent with the oncogenic role of cyclin D1 are observations that transgenic mice engineered to overexpress this cyclin in their breast tissue are prone to mammary adenocarcinomas (Wang et al., 1994), while coexpression of cyclin D1 and *myc* genes in the lymphoid tissue of transgenic mice leads to rapid development of lymphomas (Bodrug et al., 1994; Lovec et al., 1994).

Several lines of evidence suggest that particular D cyclins may have specialized functions in distinct cell types, despite the fact that they share substantial sequence homology (Matsushime et al., 1991a; Xiong et al., 1992) and a common affinity for interacting with CDK4 and CDK6 (reviewed by Sherr, 1994). Each of the D cyclins has its own distinct pattern of tissue-specific expression and accumulates with distinct kinetics following mitogen challenge, hinting at specialized roles in cell cycle progression (Matsushime et al., 1991b; Motokura et al., 1992). In addition, the various D cyclins display dramatically different patterns of expression during the terminal differentiation of muscle cells (Rao et al., 1994; Kiess et al., 1995; Skapek et al., 1995) and neurons (Tamaru et al., 1993, 1994).

To understand the distinct roles played by the D cyclins in the proliferation and differentiation of various cell types, we have used the technique of gene targeting in embryonic stem (ES) cells and created mice lacking cyclin D1, D2, or D3. In the present paper, we describe mice that lack cyclin D1. We report here that mice deficient in cyclin D1, a presumed vital component in promoting cell proliferation, are viable and show deficiencies restricted to a surprisingly narrow set of tissues.

A

WILD-TYPE GENOMIC DNA

TARGETING VECTOR
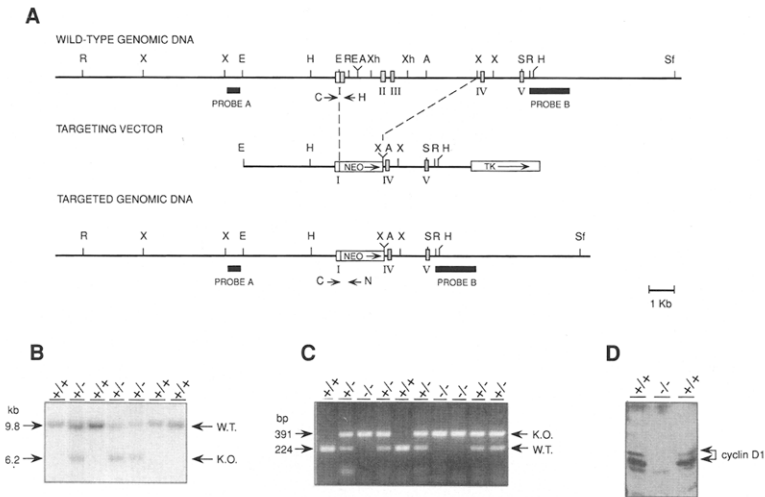
TARGETED GENOMIC DNA

B

C

D

Figure 1. Targeted Disruption of the Mouse Cyclin D1 Gene

(A) Restriction map of the mouse cyclin D1 gene, the targeting vector, and the structure of the mutated locus following the homologous recombination. The coding exons are depicted by stippled boxes and are numbered; the open box denotes the noncoding portion of the first exon. The structure of the noncoding portion of the fifth exon has not been determined. Genomic fragments used as probes for Southern blotting are depicted as closed boxes (probe A and probe B); arrows denote PCR primers (C, H, and N) used for genotyping the animals. Abbreviations and symbols: NEO, the neomycin transferase gene; TK, thymidine kinase gene; arrows show transcriptional orientation of these genes. Only relevant restriction sites are shown. The distal 4.1 kb of the presented genomic fragment (preceding the Sfil site) has not been fully restriction mapped and hence may contain additional sites. Restriction enzyme abbreviations: R, EcoRI; X, Xbal; E, Eagl; H, HindIII; A, Asp718; Xh, Xhol; S, Sall; Sf, Sfil.

(B) Southern blot analysis of genomic DNA extracted from ES cell clones. The DNA was digested with Xbal and hybridized with probe A. The sizes of wild-type (W.T.) and disrupted (K.O.) alleles are shown; the genotypes of ES cell clones are presented above the lanes.

(C) PCR amplification products of the DNA extracted from mouse tails. The sizes of amplification products of wild-type (W.T.) and disrupted (K.O.) alleles are shown; the genotypes of animals are presented above the lanes.

(D) Western blot analysis of extracts prepared from wild-type and cyclin D1$^{-/-}$ mouse embryonic fibroblasts. The blot was probed with rabbit polyclonal anti–cyclin D1 serum. Bands corresponding to cyclin D1 are indicated. The genotypes of mouse embryos from which fibroblasts were derived are shown above the lanes.

Results

Generation of Cyclin D1$^{-/-}$ Mice

To create a targeted mutation in the murine cyclin D1 gene, we isolated the mouse genomic fragment encoding cyclin D1 and determined its physical map, including exon/intron structure (Figure 1A). As is the case with its human counterpart (Motokura and Arnold, 1993), the coding sequence of the mouse cyclin D1 gene is assembled from five exons that are spread over a genomic distance of more than 7 kb (Figure 1A). The exon/intron boundaries of murine cyclin D1 gene were found to lie at precisely the same sites as those reported for the human cyclin D1 (Motokura and Arnold, 1993), D2, and D3 genes (Inaba et al., 1992).

We prepared a gene targeting construct by deleting a restriction fragment containing the coding portion of exon I as well as exons II and III and replacing it with a cassette expressing the neo gene. These exons were chosen for deletion because they encode the so-called cyclin box, a stretch of over 100 amino acid residues that is conserved among the cyclins of all eukaryotes and is believed to be essential for cyclin function (Xiong and Beach, 1991).

Following electroporation, 141 ES clones were selected using the positive–negative selection method (Mansour et al., 1988), expanded, and screened for homologous recombination events by Southern blotting analysis of their DNA (Figure 1B). Of these, 52 clones (37%) were found to be heterozygous at the cyclin D1 locus. Six ES cell clones were expanded and injected into mouse blastocysts, yielding founder chimeric mice; two ES cell clones contributed to the germline in chimeric mice, giving rise to cyclin D1 heterozygotes. Heterozygotes were bred to

produce cyclin D1$^{-/-}$ mice, which were identified by Southern blotting and polymerase chain reaction (PCR) amplification of tail DNA (Figure 1C). The absence of cyclin D1 protein in mutant mice was confirmed by Western immunoblot analysis of embryonal fibroblast lysates (Figure 1D).

Phenotype of Cyclin D1$^{-/-}$ Mice

Approximately one fourth of the offspring born in cyclin D1$^{+/-}$ × cyclin D1$^{+/-}$ crosses were found to be of the cyclin D1$^{-/-}$ genotype, indicating no significant embryonic lethality. At birth, these homozygotes appeared to be indistinguishable from wild-type and heterozygous littermates, although their weight was slightly lower. By 2 weeks of age, it became evident that the cyclin D1$^{-/-}$ mice grew more slowly; their growth retardation was most pronounced at 3 weeks of age (Figure 2A). A majority of the mutant mice died early in life, often within the first month. These were usually the smallest animals, which had failed to thrive, suggesting that starvation contributed to their death. Some of the mutant animals began to gain weight after a delay of some weeks (Figure 2A) and survived for as long as 5 months. However, they continued to show lower-than-average weight and increased mortality.

A neurological abnormality was indicated by the observation that the mutant mice retracted their limbs toward the trunk when they were lifted by their tails, in contrast with wild-type and heterozygous littermates, which invariably responded by extending their legs (Figure 2B). This abnormal leg-clasping reflex was first evident at approximately 2 weeks of age and was most pronounced by 3 weeks. It persisted in older animals but then involved clasping of only the hind limbs. The most affected of the young mutants remained in a clasped, flexed position for
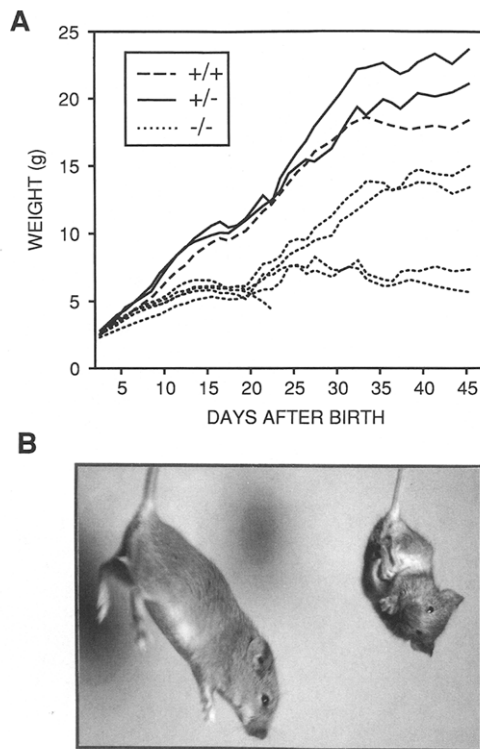
A

B

Figure 2. Phenotype of Cyclin D1$^{-/-}$ Mice

(A) Representative growth curve of wild-type, heterozygous, and cyclin D1$^{-/-}$ littermates, as indicated in the insert. One cyclin D1$^{-/-}$ mutant died at day 22; two others (with lowest weight) were moribund and were sacrificed on the last day of the observation period. An additional littermate of unknown genotype died at day 8 (data not shown).

(B) Growth retardation and abnormal leg-clasping reflex in cyclin D1$^{-/-}$ mice. When lifted by their tails, mutant mice draw their limbs toward the trunk while the wild-type mice respond by extending their legs. On the left is a wild-type mouse; on the right, a cyclin D1$^{-/-}$ mouse. Both mice were 4-week-old littermates.

a few seconds after they had been returned to the cage. They also displayed difficulty in regaining a normal body position when placed on their backs. Older mutant animals also exhibited a hunched posture. The above phenotypes were evident in more than 100 cyclin D1$^{-/-}$ mice studied, although the severity of the symptoms varied from animal to animal. Cyclin D1 heterozygotes were indistinguishable from their wild-type littermates at all stages of life.

Effects on Retinal Development

Histopathological examination of cyclin D1$^{-/-}$ mice revealed essentially normal morphogenesis in all tissues analyzed (data not shown). One clear exception was provided, however, by analysis of the retinas of these mice, which showed a dramatic reduction in cell numbers in all cell layers of the neural retina (Figures 3A and 3B). In addition, the thickness of the inner plexiform layer, which is composed of cell projections connecting ganglion cells and the inner nuclear layer, was also reduced. Nonetheless, as revealed by electron microscopy, the general architecture of the retina and retinal cell ultrastructure appeared well maintained (data not shown). One exception

to this was provided by the photoreceptor outer segments, which appeared shortened and disorganized but contained well-formed discs (data not shown). No reduction in cell numbers was found in the retinal pigmented epithelial layer. These epithelial cells were seen to have normal morphology as revealed by electron microscopy (data not shown).

The drastic reduction in retinal cell number could be explained by two mechanisms. It was possible that proliferation of cyclin D1$^{-/-}$ retinal precursor cells was impaired during embryonic development. Alternatively, the mutant mice might have initially developed normal retinas that later experienced a massive loss of cells due to a degenerative process. To distinguish between these two possibilities, we performed histologic analysis of retinas from wild-type and mutant embryos collected at 12.5, 14.5, 16.5, and 18.5 days postcoitum (dpc) and 1, 5, and 16 days postpartum (dpp) and at 5 months. The decreased number of cells in the retinas of mutant mice was observed as early as 16.5 dpc. The difference became even more apparent at 18.5 dpc and was pronounced at 1 and 5 dpp (data not shown). At 16 dpp, a time when retinal development is near completion, the mutant mice already displayed a full-blown retinal phenotype (Figures 3A and 3B) that did not differ from that seen in older mutant animals up to 5 months of age (data not shown). These observations indicated that the observed reduction of retinal cell number was due to the severely reduced ability of mutant retinal cell precursors to proliferate during embryonic development.

Electroretinographic (ERG) studies indicated that the hypoplastic retina was able to respond properly to light. Thus, electrophysiologic potentials generated in the retina were measured following exposure of mice to a short pulse of light. Two waves of electrical signaling can be observed in this procedure: the a wave arises mainly from the photoreceptors, while the b wave is generated largely by bipolar cells (Stockton and Slaughter, 1989; Steinberg et al., 1991).

Testing of cyclin D1$^{-/-}$ mice showed an approximately 10-fold reduction of their ERG amplitudes (Figures 3C and 3D). Specifically, the amplitudes of the a and b waves of cyclin D1 mutant mice were found to be 23 ± 8 μV and 92 ± 20 μV (mean ± SD), respectively, while the corresponding values for wild-type mice were 264 ± 35 μV (a wave) and 698 ± 171 μV (b wave). The observed reduction in ERG amplitudes could be accounted for by the reduction in cell number and shortened outer segments. Significantly, the mutant mice showed generally normal implicit (latency) times for both a and b waves.

Taken together, the ERG results indicated that the cells in the retinas of cyclin D1$^{-/-}$ mice are fully functional, in consonance with the generally well-maintained architecture of their retinas. By analogy to human retinopathies in which similar reduction of ERG potentials does not drastically impair vision (Berson, 1993), we assume that the residual retinal tissue of mutant mice afforded them some visual capacity. The ERG and retinal structures of cyclin D1 heterozygotes were indistinguishable from that of wild-type animals (data not shown).
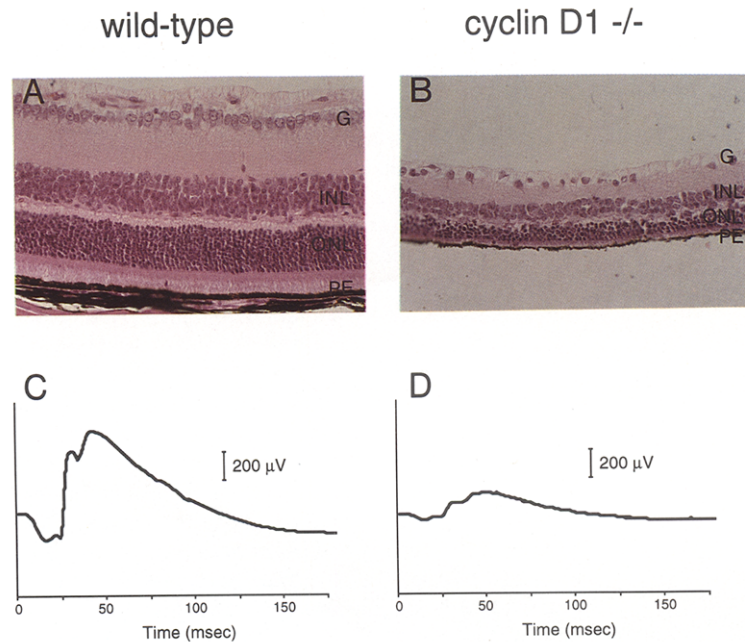
wild-type

cyclin D1 -/-

Expression of Cyclin D1 during Mouse Embryonic Development

In an attempt to understand these discrete, highly focused developmental aberrations seen in cyclin D1$^{-/-}$ mice, we examined the pattern of cyclin D1 mRNA expression during embryonal development of normal mice through use of in situ hybridization. These analyses provided a striking and unexpected explanation for the phenotypes described above. When the entire mouse embryo was examined, cyclin D1 mRNA expression was found to be most intense in the developing retina and very high in the brain (Figure 4).

The retinal expression of cyclin D1 was first observed at 11 dpc but was most pronounced at 14.5 dpc (Figures 4A and 4B). At this stage of development, the level of expression in the retina was dramatically higher than in all other tissues of the developing embryo except for the brain. Within the retina, equal intensity of staining was observed throughout the entire neural layer, while the pigmented epithelial layer showed no staining (Figure 4B).

A composite photomicrograph of a sagittal section through a 14.5 dpc mouse embryo demonstrates that an exposure time that sufficed to show an intense hybridization signal in the retina failed to reveal significant cyclin D1 expression in all other tissues (Figure 4A). We note that an intense staining of brain ventricles (Figure 4C), although lower than that seen in the retina, could not be observed in Figure 4A owing to the particular sectioning plane analyzed. Longer exposure times revealed still lower but significant levels of cyclin D1 mRNA in several other organs such as the sympathetic trunk, the lungs (Figure 4D), and the tongue (Figure 4E).

The profound effects of cyclin D1 inactivation on retinal development are most likely related to the intense expression of cyclin D1 in this tissue in wild-type mice. While no specific lesions were identified in the nervous system of mutant mice, the observed neurological phenotype and high levels of cyclin D1 in the developing brain may also be causally linked.

Proliferation of the Mammary Epithelium during Pregnancy

Mutant cyclin D1$^{-/-}$ females that survived until adulthood passed through sexual maturation. The breast tissue of these mice was able to achieve a fully developed state as judged by both histologic and whole-mount analysis (Figures 5A and 5B). The latter method makes it possible to visualize mammary epithelial duct development. As is evident from Figure 5B, the epithelial ducts of adult mutant mice were well developed and were able to form side branches.

A dramatic anomaly in mammary function first became manifest after cyclin D1$^{-/-}$ females delivered pups. These females were unable to nurse because of a defect in pregnancy-associated mammary tissue proliferation.

The mammary epithelium of female mice normally undergoes a massive expansion during pregnancy (compare Figures 5A and 5C). Specifically, the mammary epithelial ducts form side branches and develop numerous alveolar structures that cluster together to form lobules that fill the entire mammary fat pad (Figure 5E). Once secretion of milk begins, the alveoli become distended (Figure 5G).

The mammary glands of the pregnant mutant mice provided a striking contrast with the normal pregnancy-induced response. These mutant cyclin D1$^{-/-}$ glands displayed a dramatic impairment in the expansion of mammary epithelium. In particular, the development of alveolar lobules that normally occurs during pregnancy was virtually absent in the mutant mice (Figures 5D, 5F, and 5H). The number of side branches clearly increased during the pregnancy of the mutant mice, and small clusters of alveoli were formed (compare Figures 5B and 5D), but the overall
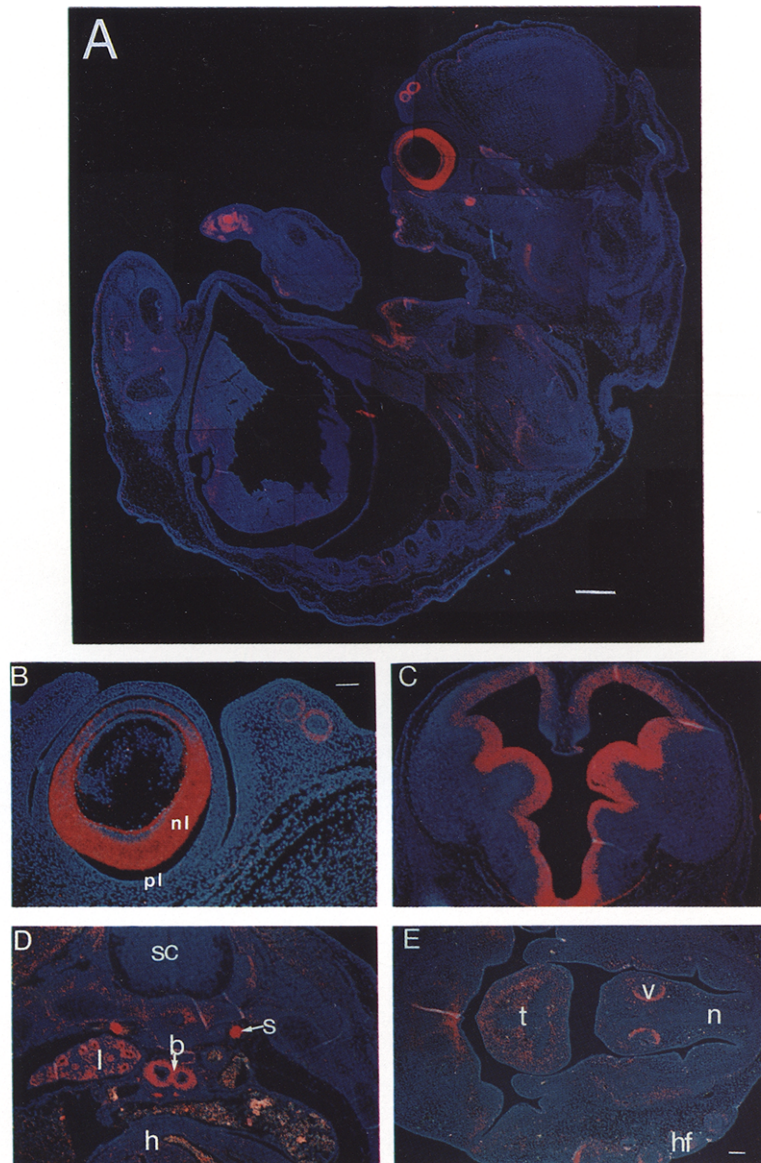
Figure 4. Expression of Cyclin D1 mRNA during Mouse Embryogenesis Detected by In Situ Hybridization

(A) Composite photomicrographs of a saggital section of a 14.5 dpc mouse embryo. All photomicrographs were taken at approximately equal exposure times.

(B) Higher magnification of the retina seen in (A). Abbreviations: nl, neural layer of the retina; pl, retinal pigmented epithelium layer.

(C) Coronal section through the brain (diencephalon) of a 13.5 dpc mouse embryo.

(D) Transverse section through the spinal cord and intercostal region of a 14.5 dpc mouse embryo. Abbreviations: b, bronchus; h, heart; l, lung; s, sympathetic ganglion; sc, spinal cord.

(E) Coronal section through the oral and nasal cavities of a 12 dpc mouse embryo. Abbreviations: hf, hair follicle; n, nasal septum; t, tongue; v, vomeronasal organ (Jacobson's organ).

Scale bar in (A), 500 μm; in (B), 100 μm; in (C)–(E) as represented in (E), 100 μm. Specimens were photographed by double exposure using dark-field illumination with a red filter and Hoechst epifluorescence optics. The blue color represents the Hoechst staining of cell nuclei, and the red represents the cyclin D1 hybridization signal.

rate of expansion was inconsequential when compared with the pregnancy-associated epithelial proliferation seen in the mammary glands of wild-type mice (Figures 5E and 5F).

Ovarian Steroid Hormones and Estrogen Receptors

The ovarian steriod hormones estrogen and progesterone are largely responsible for inducing the lobuloalveolar development of the breast during pregnancy (Bresciani, 1968). Thus, it was possible that the failure of mammary proliferation in the cyclin D1$^{-/-}$ mutant mice was due to inadequate levels of these hormones. This was rendered less likely by the observed capacity of mutant mice to become pregnant and to bear offspring to full term and by the normal gross and microscopic structure of their uteri (data not shown).

We reinforced this conclusion by measuring the levels of estrogen and progesterone in the peripheral blood of pregnant (16.5 dpc) mice and at 1 day after delivery in cyclin D1$^{-/-}$ and wild-type females. We chose 16.5 dpc because blood progesterone levels are known to peak at this time (Barkley et al., 1979). We found that the hormone levels in the two types of mice were comparable (Table 1) and fell within the normal range (Barkley et al., 1979).

Much of the hormone responsiveness is mediated by the estrogen receptor (ER) expressed by cells of the mammary gland. The expression of this receptor is required for both the estrogen-induced proliferation of the mammary epithelium and for responsiveness to progesterone (Haslam, 1988a, 1989). For this reason, we compared the proportion of ER-positive cells in the mammary glands of nulliparous and pregnant (16.5 dpc) mice. In the immunoperoxidase method that we used to detect the ER, the intensity of staining quantitatively reflects the content of ER in the nucleus (Bacus et al., 1988), thereby allowing a rough estimate of the amount of ER present in cell nuclei. When

Table 1. The Levels of Steroid Hormones

| Steroid Hormone	Wild Type	Cyclin D1⁻/⁻
Progesterone, 16.5 dpc	97.6 ± 14.2	78.6 ± 13.1
Progesterone, 1 day after delivery	5.0 ± 1.4	4.1 ± 1.0
Estradiol, 16.5 dpc	38.4 ± 7.7	35.6 ± 4.3
Estradiol, 1 day after delivery	29.2 ± 7.1	34.2 ± 12.5

The concentrations of progesterone and estradiol were determined in peripheral blood of 16.5 dpc pregnant mice (16 dpc) or 1 day after delivery as described in Experimental Procedures. The concentrations are presented as means ± SD and are expressed in nanograms per milliliter for progesterone and picograms per milliliter for estradiol. The number of animals analyzed: n = 6 for wild type, 16.5 dpc; n = 4 for cyclin D1⁻/⁻, 16.5 dpc; n = 4 for wild type, 1 day after delivery; n = 2 for cyclin D1⁻/⁻, 1 day after delivery.

normal and mutant breast tissue was compared in this way, no apparent differences were observed in either the fraction of ER-positive cells or in the intensity of nuclear staining (data not shown).

We concluded that the mammary epithelial cell proliferation defect seen in the mutant mice during pregnancy could not be ascribed either to the deficiency of circulating ovarian steroid hormones or to the absence of ER, but reflected instead a defect in the hormone responsiveness of the target organ.

Discussion

The functions of the three mammalian D-type cyclins remain incompletely understood. Of these three, cyclin D1 is the best studied. In vitro inactivation of cyclin D1 by injection of antibodies or antisense plasmids into cultured fibroblasts has been found to block proliferation of these cells. In addition, expression of cyclin D1 has been documented in almost all nontransformed cell lines examined (reviewed by Sherr, 1994). For these reasons, we anticipated that a homozygous inactivation of the cyclin D1 gene in the mouse germline would severely compromise cell proliferation in the developing embryo, leading in turn to early embryonic lethality.
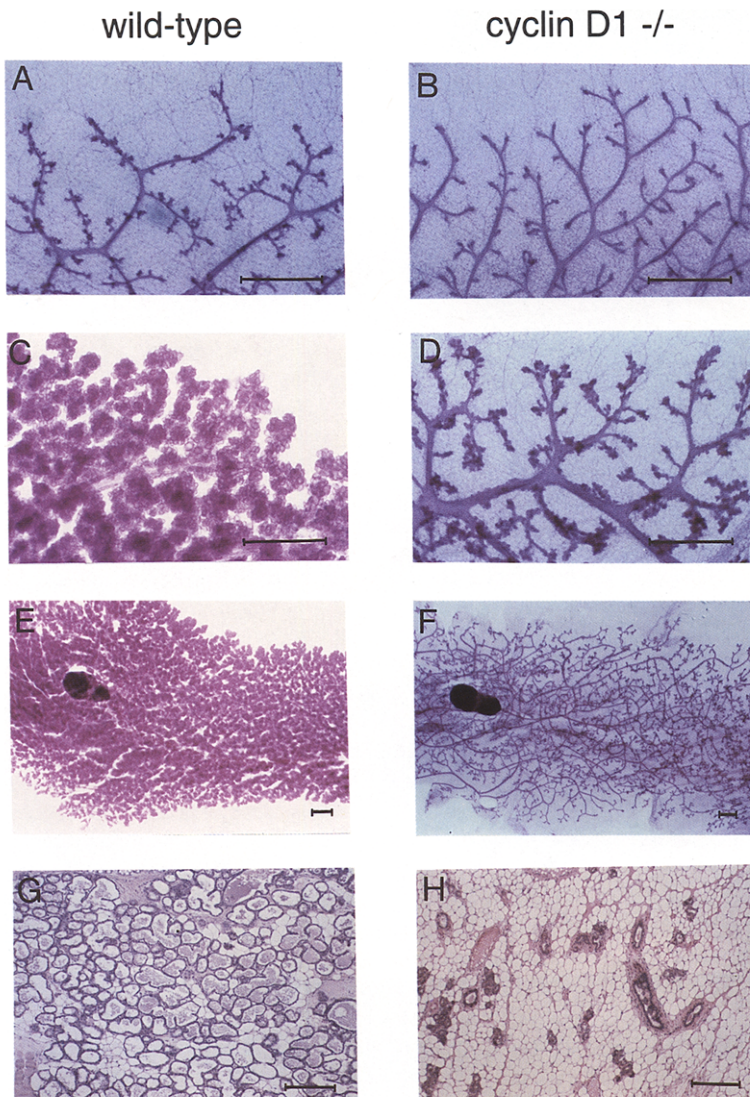
Figure 5. Impaired Mammary Epithelial Expansion during Pregnancy in Cyclin D1⁻/⁻ Mice

The whole-mount (A–F) and histologic (G and H) appearance of the mammary glands derived from 18- to 22-week-old wild-type (A, C, E, and G) and cyclin D1⁻/⁻ (B, D, F, and H) mice. The whole mounts of inguinal mammary glands were prepared as described in Experimental Procedures, and the epithelial component was stained with carmine red. The paraffin histologic sections (G and H) were stained with hematoxylin and eosin. The bar denotes 1 mm (A–F) or 0.2 mm (G and H).
(A) Nulliparous wild-type mouse.
(B) Nulliparous mutant mouse.
(C and E) Wild-type mouse, 1.5 day after delivery.
(D and F) Mutant mouse, 1 day after delivery.
(G) Wild-type mouse, 1 day after delivery.
(H) Mutant mouse, 1 day after delivery.

The observed limited effects of the cyclin D1$^{-/-}$ genotype were therefore unexpected. Cyclin D1 is apparently dispensable for the proliferation of the majority of tissues in which, we speculate, other D-type cyclins provide substitutes for its functions. We discuss three discernible consequences of cyclin D1 loss below.

The Neurological Phenotype

The behavioral phenotype observed in cyclin D1$^{-/-}$ mice, in particular the abnormal limb reflex (Figure 2B), provides clear indication of an abnormality in the functioning of the nervous system. Clasping of the limbs has been reported in several spontaneously arising neurologic mutants and in mutants generated by targeted disruption of genes critical for the development or functioning of neurons (Urbanek et al., 1994, and references therein). While no obvious histopathological abnormalities were found in the nervous system of cyclin D1$^{-/-}$ mice, minor neuroanatomical defects might suffice to cause these neurological symptoms (for example, Klein et al., 1994); such lesions would have escaped our attention.

Our in situ hybridization analysis did demonstrate very high expression of cyclin D1 mRNA in the developing brain (Figure 4C) and significant levels in the developing sympathetic trunk (Figure 4D), but only very low levels in the adult brain (data not shown). Others have reported that expression of cyclin D1 increases during the maturation of rat brain (Tamaru et al., 1993). The precise impact of cyclin D1 deficiency on the functional development of the nervous system will remain obscure until specific neuroanatomical lesions can be identified in cyclin D1$^{-/-}$ animals.

The Retinal Phenotype

In striking contrast with the great majority of mouse tissues in which loss of cyclin D1 is inconsequential for development, we find that the retinal precursor cells are critically dependent on cyclin D1 for their proliferation. Independent of this observation was the finding of extremely high levels of cyclin D1 expression in this tissue. As is evident from Figure 4A, the level of cyclin D1 mRNA in the developing retina is dramatically higher than that seen in all other tissues during a period when many embryonal tissues are known to be in a highly proliferative state (Kaufman, 1992). These observations provide us with a rationale for the described retinal phenotype. Thus, we speculate that the proliferation of cells in the developing neural retina is driven by and indeed requires unusually high levels of cyclin D1.

We are also struck by the fact that a rare malignancy of this tissue, retinoblastoma, led to the discovery of important mechanisms regulating progress of the cell through the G1 phase of the cell cycle. Cyclin D1, working with its partner CDKs, is known to be responsible for triggering pRB phosphorylation and functional inactivation (reviewed by Weinberg, 1995). Furthermore, cyclin D1 is able to bind pRB directly (reviewed by Sherr, 1994). Given this connection, it seems more than a coincidence that two independent lines of experimentation, one studying the human Rb gene and the other the mouse cyclin D1 gene, have converged on this small, highly specialized tissue.

Recognizing the clear differences between human and mouse retinas, notably the lack of retinoblastomas in Rb$^{-/-}$ mice (Clarke et al., 1992; Jacks et al., 1992; Lee et al., 1992), we suggest that this apparent coincidence may reflect some common underlying molecular process responsible for regulating retinal cell proliferation and differentiation. For example, retinal cells may require especially high levels of pRB to block G1 progression prior to end-stage differentiation. Retinal cells may also express especially high levels of cyclin D1 to neutralize pRB when proliferation is required during normal development. Such high dependence on pRB may in turn create a special predilection for malignant retinal cell transformation should pRB function be compromised by Rb gene mutation.

Breast Epithelial Phenotype

Most striking was the severe impairment of mammary epithelial cell proliferation in mutant mice during pregnancy. As is the case in humans, the intense proliferation of the mouse mammary epithelium occurs during two well-defined periods of life, namely, ductal elongation at puberty and ductal side branching and lobuloalveolar formation during pregnancy. The ductal elongation seen at puberty is directly stimulated by estrogen but is refractory to progesterone treatment (Haslam, 1988b).

Once mice reach sexual maturity and their breast tissue becomes fully developed, the mammary epithelial cells acquire progesterone receptors and no longer proliferate in response to estrogen alone. Indeed, they now require both estrogen and progesterone for their proliferation, which results in ductal side branching and lobuloalveolar development during pregnancy (Wang et al., 1990). We also note that expression of the progesterone receptor is induced by the action of estrogen in adult but not developing mammary epithelium (Haslam, 1988a).

It is clear that the mammary glands of cyclin D1$^{-/-}$ mutant females attain an essentially fully developed state during sexual maturation, as evidenced by both whole-mount analysis (Figure 5B) and histology (data not shown). The possibility of some subtle retardation of this development could not be ruled out in our study owing to the limited number of animals analyzed and their mixed genetic background. A clear and dramatic impairment of mammary gland proliferation is first observed during pregnancy. While the mammary epithelium of wild-type animals develops numerous side branches and forms large clusters of alveoli (Figures 5C, 5E, and 5G), this pregnancy-associated response in the mutant mice is dramatically reduced (Figures 5D, 5F, and 5H).

Numerous hormones have been found to act in concert to induce full development and lactation of the mammary gland during pregnancy. Included here are the ovarian steroids estrogen and progesterone, the pituitary hormones prolactin and growth hormone, as well as adrenal steroids (Nandi, 1958). However, the critical role in stimulating mammary epithelial proliferation during this period has been ascribed to the ovarian steroids (Haslam, 1988b; Wang et al., 1990).

As reported here, the observed phenotype cannot be ascribed to the absence of ovarian hormones in the pregnant mutant females or to the lack of ERs in their mammary

goat anti-rabbit IgG (Jackson ImmunoResearch) was used as a secondary antibody at 1:5000 dilution followed by enhanced chemiluminescence (ECL) detection (Amersham).

Histology and Electron Microscopy

For histology, mice were perfused with Bouin's fixative (Sigma). Tissues were dissected, fixed further in Bouin's fixative, processed, and embedded in paraffin using standard procedures. Sections (6 μm) were cut and stained with hematoxylin and eosin. Alternatively, tissues were fixed in 4% formaldehyde in 0.1 M phosphate buffer, infiltrated with 30% sucrose in the same buffer, mounted in OCT medium (Miles), and snap-frozen in isopentane. Cryostat sections (10 μm thick) were cut and stained with hematoxylin and eosin.

For electron microscopy, enucleated eyes were fixed overnight in 1% formaldehyde and 2.5% glutaraldehyde in phosphate-buffered saline (PBS). The eye cups were then postfixed in osmium tetroxide and embedded in Epon. Ultrathin sections (60–80 nm) were cut, stained with uranyl acetate and lead citrate, and viewed under a JEOL 100C transmission electron microscope.

ERG Testing

Mice were adapted to the dark for 12 hr before testing. Testing was conducted essentially as described previously (Olsson et al., 1992), except that electrodes were placed in direct contact with the cornea. ERGs were elicited from one eye of each animal with 0.1 Hz, 10 μs flashes of bright white light. Signals were differentially amplified, digitized, and filtered. We tested five wild-type and five cyclin D1$^{-/-}$ mice. For each animal analyzed, four separate responses were generated, and a composite tracing was averaged by computer. Representative tracings for each genotype are presented in Figures 3C and 3D. With this setup, the a wave amplitudes in wild-type adult pigmented mice fall in the range between 100–300 μV, while b wave amplitudes fall in the range of 400–1200 μV. The implicit (flash onset to peak) times are in the range of 15–30 ms for the a waves and 45–75 ms for the b waves (T. L. and B. Pawlyk, unpublished data).

In Situ Hybridization

In situ hybridizations were performed on mouse embryos from 9 to 14.5 dpc and on adult tissues as previously described (Wilkinson, 1993; Parker et al., 1995). Standard protocols for collecting, embedding, and sectioning the tissues were employed. pBluescript mouse cyclin D1 cDNA (Matsushime et al., 1991b) was linearized with HindIII, and antisense transcripts were generated using T3 polymerase. Specimens were hybridized with [^{35}S]UTP-labeled riboprobes.

Mammary Gland Whole Mounts

Inguinal mammary glands were dissected, spread onto a glass slide, fixed in a 1:3 mixture of glacial acetic acid:ethanol, hydrated, stained overnight in 0.2% carmine (Sigma) and 0.5% AlK(SO$_4$)$_2$, dehydrated in graded solutions of ethanol, and cleared in toluene and methyl salicylate essentially as described previously (Wang et al., 1990).

Measurement of Serum Steroid Hormone Levels

Peripheral blood was collected from the orbital venous sinus of pregnant mice (16.5 dpc) or 1 day after delivery. Serum was collected by centrifugation and kept at −80°C. Progesterone and estradiol levels were measured by immunoassay using rabbit polyclonal antibodies generated by the Reproductive Endocrine Unit Laboratory at Massachusetts General Hospital (Boston, MA) as described previously (Hall et al., 1992).

ER Immunocytochemistry

Inguinal mammary glands were dissected from nulliparous or pregnant (16.5 dpc) mice, mounted in OCT compound (Miles), and snap-frozen in isopentane. Cryostat sections (6 μm) were fixed for 5 min at room temperature in 10% formalin in PBS, followed by methanol for 3–5 min at −10°C, acetone for 1–3 min at −10°C, and two rinses in PBS for 5 min each. The immunoperoxidase staining was performed as described previously (Haslam and Nummy, 1992) with the exception that the ImmunoPure metal-enhanced DAB substrate kit (Pierce) was used for chromagen development. Nuclei were counterstained with 1% methyl green for 1 min. Anti-ER monoclonal antibody H222 was a gift of Abbott Labs.

References

Adnane, J., Gaudray, P., Simon, M.-P., Simony-Lafontaine, J., Jeanteur, P., and Theillet, C. (1989). Proto-oncogene amplification and human breast cancer tumor phenotype. Oncogene 4, 1389–1395.

Bacus, S., Flowers, J. L., Press, M. F., Bacus, J. W., and McCarty, K., Jr. (1988). The evaluation of estrogen receptor in primary breast carcinoma by computer-assisted image analysis. Am. J. Clin. Pathol. 90, 233–239.

Barkley, M. S., Geschwind, I. I., and Bradford, G. E. (1979). The gestational pattern of estradiol, testosterone, and progesterone secretion in selected strains of mice. Biol. Reprod. 20, 733–738.

Bartkova, J., Lukas, J., Müller, H., Lützhoft, D., Strauss, M., and Bartek, J. (1994). Cyclin D1 protein expression and function in human breast cancer. Int. J. Cancer 57, 353–361.

Berson, E. L. (1993). Retinitis pigmentosa: Friedenwald lecture. Invest. Ophthalmol. Vis. Sci. 34, 1659–1676.

Bodrug, S. E., Warner, B. J., Bath, M. L., Lindeman, G. J., Harris, A. W., and Adams, J. M. (1994). Cyclin D1 transgene impedes lymphocyte maturation and collaborates in lymphomagenesis with the myc gene. EMBO J. 13, 2124–2130.

Bresciani, F. (1968). Topography of DNA synthesis in the mammary gland of the C3H mouse and its control by ovarian hormones. Cell Tissue Kinet. 1, 51–63.

Buckley, M. F., Sweeney, K. J. E., Hamilton, J. A., Sini, R. L., Manning, D. L., Nicholson, R. I., deFazio, A., Watts, C. K. W., Musgrove, E. A., and Sutherland, R. L. (1993). Expression and amplification of cyclin genes in human breast cancer. Oncogene 8, 2127–2133.

Clarke, A. R., Maandag, E. R., van Roon, M., van der Lugt, N. M. T., van der Valk, M., Hooper, M. L., Berns, A., and te Riele, H. (1992). Requirement for a functional Rb-1 gene in murine development. Nature 359, 328–330.

Gossler, A., Doetschman, T., Korn, R., Serfling, E., and Kemler, R. (1986). Transgenesis by means of blastocyst-derived embryonic stem cell lines. Proc. Natl. Acad. Sci. USA 83, 9065–9069.

Hall, J. E., Schoenfeld, D. A., Martin, K. A., and Crowley, W., Jr. (1992). Hypothalamic gonadotropin-releasing hormone secretion and follicle-stimulating hormone dynamics during the luteal–follicular transition. J. Clin. Endocrinol. Metab. 74, 600–607.

Haslam, S. Z. (1988a). Acquisition of estrogen-dependent progesterone receptors by normal mouse mammary gland: ontogeny of mammary progesterone receptors. J. Steroid Biochem. 31, 9–13.

Haslam, S. Z. (1988b). Progesterone effects on deoxyribonucleic acid synthesis in normal mouse mammary glands. Endocrinology 122, 464–470.

Haslam, S. Z. (1989). The ontogeny of mouse mammary gland responsiveness to ovarian steroid hormones. Endocrinology 125, 2766–2772.

Haslam, S. Z., and Nummy, K. A. (1992). The ontogeny and cellular distribution of estrogen receptors in normal mouse mammary gland. J. Steroid Biochem. Mol. Biol. 42, 589–595.

Inaba, T., Matsushime, H., Valentine, M., Roussel, M. F., Sherr, C. J., and Look, A. T. (1992). Genomic organization, chromosomal localization, and independent expression of human cyclin D genes. Genomics 13, 565–574.

Jacks, T., Fazeli, A., Schmitt, E. M., Bronson, R. T., Goodell, M. A., and Weinberg, R. A. (1992). Effects of an Rb mutation in the mouse. Nature 359, 295–300.

Kaufman, M. H. (1992). The Atlas of Mouse Development (London: Academic Press).

Kiess, M., Gill, R. M., and Hamel, P. A. (1995). Expression of the positive regulator of cell cycle progression, cyclin D3, is induced during differentiation of myoblasts into quiescent myotubes. Oncogene 10, 159–166.

Klein, R., Silos-Santiago, I., Smeyne, R. J., Lira, S. A., Brambilla, R., Bryant, S., Zhang, L., Snider, W. D., and Barbacid, M. (1994). Disruption of the neurotrophin-3 receptor gene trkC eliminates Ia muscle afferents and results in abnormal movements. Nature 368, 249–251.

Lee, E. Y.-H. P., Chang, C.-Y., Hu, N., Wang, Y.-C. J., Lai, C.-C., Herrup, K., Lee, W.-H., and Bradley, A. (1992). Mice deficient for Rb are nonviable and show defects in neurogenesis and haematopoesis. Nature 359, 288–294.

Lovec, H., Grzeschiczek, A., Kowalski, M. B., and Moroy, T. (1994). Cyclin D1/bcl-1 cooperates with myc genes in the generation of B-cell lymphoma in transgenic mice. EMBO J. 13, 3487–3495.

Mansour, S. L., Thomas, K. R., and Capecchi, M. R. (1988). Disruption of the proto-oncogene int-2 in mouse embryo-derived stem cells: a general strategy for targeting mutations to non-selectable genes. Nature 336, 348–352.

Matsushime, H., Roussel, M. F., and Sherr, C. J. (1991a). Novel mammalian cyclins (CYL genes) expressed during G1. Cold Spring Harbor Symp. Quant. Biol. 56, 69–74.

Matsushime, H., Roussel, M. F., Ashum, R. A., and Sherr, C. J. (1991b). Colony-stimulating factor 1 regulates novel cyclins during the G1 phase of the cell cycle. Cell 65, 701–713.

Motokura, T, and Arnold, A. (1993). PRAD1/cyclin D1 proto-oncogene: genomic organization, 5′DNA sequence, and sequence of a tumor-specific rearrangement breakpoint. Genes Chromosom. Cancer 7, 89–95.

Motokura, T., Bloom, T., Goo-Kim, H., Jüppner, H., Ruderman, J. V., Kronenberg, H. M., and Arnold, A. (1991). A novel cyclin encoded by a bcl1-linked candidate oncogene. Nature 350, 512–515.

Motokura, T., Keyomarsi, K., Kronenberg, H. M., and Arnold, A. (1992). Cloning and characterization of human cyclin D3, a cDNA closely related in sequence to the PRAD1/Cyclin D1 proto-oncogene. J. Biol. Chem. 267, 20412–20415.

Musgrove, E. A., Hamilton, J. A., Lee, C. S. L., Sweeney, K. J. E., Watts, C. K. W., and Sutherland, R. L. (1993). Growth factor, steroid, and steroid antagonist regulation of cyclin gene expression associated with changes in T-47D human breast cancer cell cycle progression. Mol. Cell. Biol. 13, 3577–3587.

Musgrove, E. A., Lee, C. S., Buckley, M. F., and Sutherland, R. L. (1994). Cyclin D1 induction in breast cancer cells shortens G1 and is sufficient for cells arrested in G1 to complete the cell cycle. Proc. Natl. Acad. Sci. USA 91, 8022–8026.

Nandi, S. (1958). Endocrine control of mammary-gland development and function in the C3H/He Crgl mouse. J. Natl. Cancer Inst. 21, 1040–1051.

Olsson, J. E., Gordon, J. W., Pawlyk, B. S., Roof, D., Hayes, A., Molday, R. S., Mukai, S., Cowley, G. S., Berson, E. L., and Dryja, T. P. (1992). Transgenic mice with a rhodopsin mutation (Pro23His): a mouse model of autosomal dominant retinitis pigmentosa. Neuron 9, 815–830.

Parker, S. B., Eichele, G., Zhang, P., Rawls, A., Sands, A. T., Bradley, A., Olson, E. N., Harper, J. W., and Elledge, S. J. (1995). p53-

independent expression of p21Cip1 in muscle and other terminally differentiating cells. Science 267, 1024–1027.

Rao, S. S., Chu, C., and Kohtz, D. S. (1994). Ectopic expression of cyclin D1 prevents activation of gene transcription by myogenic basic helix-loop-helix regulators. Mol. Cell. Biol. 14, 5259–5267.

Robertson, E. J. (1987). Embryo-derived stem cell lines. In Teratocarcinomas and Embryonic Stem Cells, E. J. Robertson, ed. (Oxford: Oxford University Press), pp. 71–112.

Schuuring, E., Verhoeven, E., van Tinteren, H., Peterse, J. L., Nunnink, B., Thunnissen, F. B., Devilee, P., Cornelisse, C. J., van de Vijver, M. J., Mooi, W. J., and Michalides, R. J. A. M., (1992). Amplification of genes within the chromosome 11q13 region is indicative of poor prognosis in patients with operable breast cancer. Cancer Res. 52, 5229–5234.

Sherr, C. J. (1994). G1 phase progression: cycling on cue. Cell 79, 551–555.

Skapek, S. X., Rhee, J., Spicer, D. B., and Lassar, A. B. (1995). Inhibition of myogenic differentiation in proliferating myoblasts by cyclin D1-dependent kinase. Science 267, 1022–1024.

Steinberg, R. H., Frishman, L. J., and Sieving, P. A. (1991). Negative components of the electroretinogram from proximal retina and photoreceptor. In Progress in Retinal Research, N. N. Osborne and G. J. Chader, eds. (Oxford: Pergamon), pp. 121–160.

Stockton, R. A., and Slaughter, M. M. (1989). B-wave of the electroretinogram: a reflection of ON bipolar cell activity. J. Gen. Physiol. 93, 101–122.

Sutherland, R. L., Watts, C. K. W., and Musgrove, E. A. (1993). Cyclin gene expression and growth control in normal and neoplastic human breast epithelium. J. Steroid Biochem. Mol. Biol. 47, 99–106.

Tamaru, T., Trigun, S. K., Okada, M., and Nakagawa, H. (1993). Identification of cells expressing a D type G1 cyclin in matured brain: implication for its role in neuronal function. Neurosci. Lett. 153, 169–172.

Tamaru, T., Okada, M., and Nakagawa, H. (1994). Differential expression of D type cyclins during neuronal maturation. Neurosci. Lett. 168, 229–232.

Urbanek, P., Wang, Z. Q., Fetka, I., Wagner, E. F., and Busslinger, M. (1994). Complete block of early B cell differentiation and altered patterning of the posterior midbrain in mice lacking Pax5/BSAP. Cell 79, 901–912.

Wang, S., Counterman, L. J., and Haslam, S. Z. (1990). Progesterone action in normal mouse mammary gland. Endocrinology 127, 2183–2189.

Wang, T. C., Cardiff, R. D., Zukerberg, L., Lees, E., Arnold, A., and Schmidt, E. V. (1994). Mammary hyperplasia and carcinoma in MMTV-cyclin D1 transgenic mice. Nature 369, 669–671.

Watts, C. K., Sweeney, K. J., Warlters, A., Musgrove, E. A., and Sutherland, R. L. (1994). Antiestrogen regulation of cell cycle progression and cyclin D1 gene expression in MCF-7 human breast cancer cells. Breast Cancer Res. Treat. 31, 95–105.

Weinberg, R. A. (1995). The retinoblastoma protein and cell cycle control. Cell 81, 323–330.

Wilkinson, D. G. (1993). In situ hybridization. In Essential Developmental Biology, C. D. Stern and P. W. H. Holland, eds. (New York: Oxford University Press), pp. 257–263.

Xiong, Y., and Beach, D. (1991). Population explosion in the cyclin family. Curr. Biol. 1, 362–364.

Xiong, Y., Menninger, J., Beach, D., and Ward, D. C. (1992). Molecular cloning and chromosomal mapping of CCND genes encoding human D-type cyclins. Genomics 13, 575–584.